Synthesis and Intramolecular Charge Separation of Fixed-Distance Triads Consisting of Zinc Porphyrin, Metal-Free Porphyrin, and Electron-Accepting Diimide Moiety

Atsuhiro OSUKA,* Run-Ping ZHANG, Kazuhiro MARUYAMA, Takeshi OHNO,† and Koichi NOZAKI†
Department of Chemistry, Faculty of Science, Kyoto University, Kyoto 606
†Department of Chemistry, College of General Education, Osaka University, Toyonaka 560
(Received June 22, 1993)

Synthesis of fixed-distance triads consisting of zinc porphyrin (ZnP), metal-free porphyrin (H_2P), and pyromellitimide (PIm) or 1,4:5,8-naphthalenetetracarboximide (NIm) is described. The ZnP and H_2P moieties are bridged by aromatic spacers such as 1,4-phenylene, 4,4′-biphenylylene, methylenebis(1,4-phenylene), and bicyclo[2.2.2]octane-1,4-diylbis(1,4-phenylene) groups. The steady-state fluorescence spectra indicated the occurrence of intramolecular singlet-singlet energy transfer form the ZnP to the H_2P. Formation of long-lived charge-separated states $(ZnP)^+$–H_2P–$(PIm)^-$ and $(ZnP)^+$–H_2P–$(NIm)^-$ with lifetimes of 0.14—80 μs in THF was observed by nanosecond to microsecond transient absorption spectroscopy. The lifetimes of the $(ZnP)^+$–H_2P–$(Im)^-$ states depend on the distances between the charged sites as well as the energy gaps between the ion pair and the ground state.

The X-ray crystallographic studies of the bacterial reaction center (RC) have shown that four bacteriochlorophylls, two bacteriopheophytins, two quinones, and an iron(II) are arranged in an approximately C_2 symmetric structure.[1,2] In RC, the initial electron transfer (ET) occurs on a 2—3 picosecond time scale, while subsequent electron-transfer reactions occur on a time range from hundreds of picoseconds to microseconds, leading to a long-lived ion pair (IP) state in virtually quantitative yield.[3] In recent years, considerable effort has been devoted to studies of photoinduced intramolecular ET in multicomponent molecules.[4,5] Generation of a long-lived IP state via initial ET within the singlet manifold is apparently an important issue in this field. As part of a program on artificial models for photosynthetic reaction center,[6] our laboratory has been involved in the preparation and the study of models which are capable of producing long-lived charge-separated states from singlet excited states in high quantum yields.

In this paper, we report the synthesis of triads **1a**—**d** and **2a**—**d** (Chart 1) consisting of zinc porphyrin (ZnP), metal-free porphyrin (H_2P), and electron-accepting diimide moiety (Im).[7] We also report the formation of long-lived charge-separated states upon photoexcitation of these triads. Our design of **1** and **2** is based on the following characteristic features of the respective components: firstly, there exists an energy gradient (Scheme 1), which is favorable for the formation of a charge-separated state $(ZnP)^+$–H_2P–$(Im)^-$ from $^1(ZnP)^*$–H_2P–Im. Secondly, a pyromellitimide moiety (PIm) is a stable, effective electron acceptor toward the singlet excited state of porphyrin[8] and has been proven to be quite useful for analysis of ET kinetics because of the characteristic sharp absorption at ca. 715 nm due to $(PIm)^-$.[7,8—12] 1,4:5,8-Naphthalenetetracarboximide (NIm) is a stronger electron acceptor than PIm, and the absorption spectrum of $(NIm)^-$ is also well-characterized. It is expected that the energy levels of ion-pair states, ZnP–$(H_2P)^+$–$(NIm)^-$ and $(ZnP)^+$–H_2P–$(NIm)^-$, are lower than those of the corresponding states, ZnP–$(H_2P)^+$–$(PIm)^-$ and $(ZnP)^+$–H_2P–$(PIm)^-$, respectively.

Although the linkage between the H_2P and Im is flexible, the center-to-center distance is restricted to ca. 13 Å. The ZnP and H_2P moieties are connected by aromatic spacers such as 1,4-phenylene, 4,4′-biphenylylene, methylenebis(1,4-phenylene), and bicyclo[2.2.2]-octane-1,4-diylbis(1,4-phenylene) groups; the center-to-center distances between ZnP and H_2P are also fixed to 13.0, 17.2, 16.0, and 21.7 Å, respectively.

Results and Discussion

Synthesis of Triads. Triads **1b**—**d** were prepared by partial metalation of diporphyrins **7b**—**d**. The synthesis of **7b**—**d** is outlined in Scheme 2. Acid-catalyzed condensation[13] of 4-methylbenzaldehyde and monoprotected aromatic aldehydes **4b**—**d** with bis(3-hexyl-4-methyl-2-pyrrolyl)methane (**3**)[14] in the presence of trichloroacetic acid followed by oxidation with *p*-chloranil and acidic deprotection provided formyl-substituted porphyrins **5b**—**d** in 22—28% yields. Similar condensation of **5b**—**d** and pyromellitimide-linked aldehyde **6** with **3** gave the diporphyrins **7b**—**d** in 7—45% yields based on the amounts of **5b**—**d** used.[15] Triads **9b**—**d** were prepared similarly from the condensation of **5b**—**d** and aldehyde **8** with **3** in 15—40% yields (Chart 2).

Treatment of **7b** with a dilute MeOH solution of zinc acetate in CH_2Cl_2 followed by flash column chromatography on silica gel gave its two monozinc complexes. These two compounds exhibit the same mass 2043 (M^++2) (FAB, *m*-nitrobenzyl alcohol matrix, 10 keV) and display quite similar ^1H NMR spectra to each other. In every experiment, one isomer (which moves faster on TLC than the other) was obtained in a more amount than the other (in an about 2:1 ratio). The

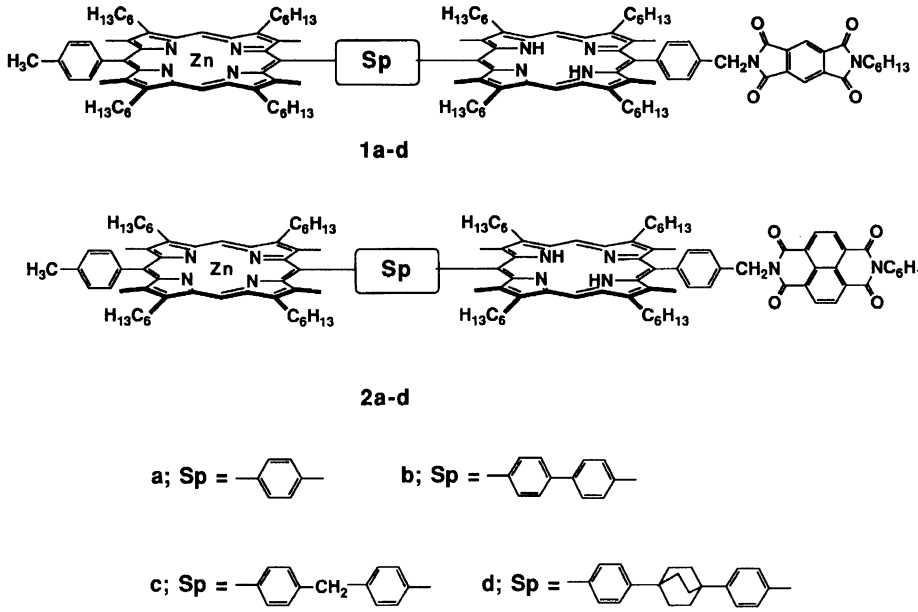

Chart 1. Structures of **1** and **2** studied in this paper.

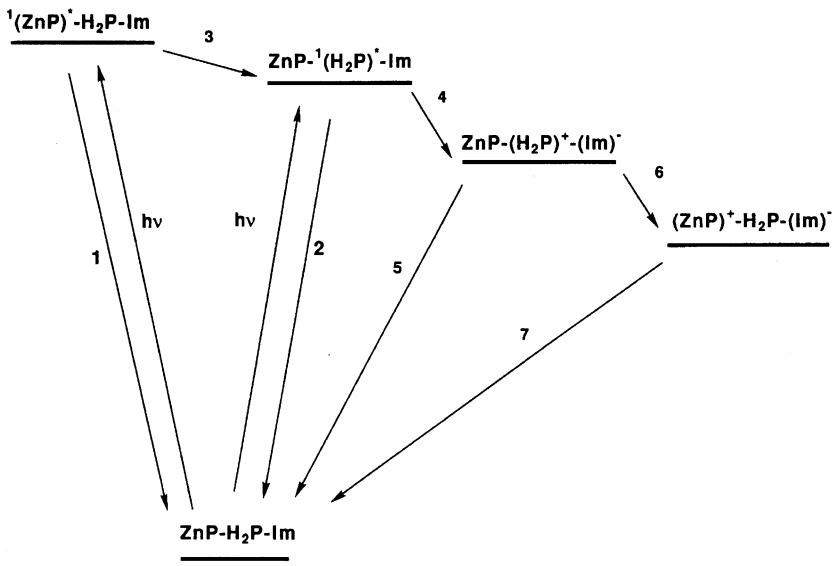

Scheme 1. Reaction scheme for triads **1a** (Im=PIm) and **2a** (Im=NIm). Energy levels are as follows; $^1(ZnP)^*$, 2.13 eV; $^1(H_2P)^*$, 1.97 eV; ZnP–$(H_2P)^+$–$(PIm)^-$, 2.00 eV; ZnP–$(H_2P)^+$–$(NIm)^-$, 1.64 eV; $(ZnP)^+$–H_2P–$(PIm)^-$, 1.72 eV; $(ZnP)^+$–H_2P–$(NIm)^-$, 1.48 eV. Energy levels of the ion pair states were calculated on the basis of the redox potentials of the chromophores measured in DMF and work terms due to static Columbic stabilization energy between the charged states.

two monozinc complexes were identified by their steady-state fluorescence spectra. In comparison of these fluorescence spectra (Fig. 1), the intensity of the emission due to the $^1(H_2P)^*$ at 630 and 690 nm is less in the major isomer, while that due to the $^1(ZnP)^*$ at 580 and 630 nm is less in the minor isomer. In these monozinc complexes, it is expected that the fluorescence of the ZnP is quenched through intramolecular singlet-singlet energy transfer to the H_2P[11,16] and that the fluorescence of the porphyrin proximal to the attached diimide is quenched through intramolecular electron transfer. Taking these into account, the assignment is straightforward; the major one is **1b**, and the minor is the other monozinc complex in which the proximal porphyrin site is metalated. Nagata reported that when 2,6-bis(benzyloxy)phenyl groups or 2,6-dimethoxyphenyl groups exist in the distal porphyrin site, the zinc-metalation at the proximal site was predominant,[14] but in the present system the distal site was preferentially metalated.

Trials **1a** and **2a** were prepared by a different route, because the two monozinc complexes formed by partial metalation of **7a** or **9a** were not separable by flash col-

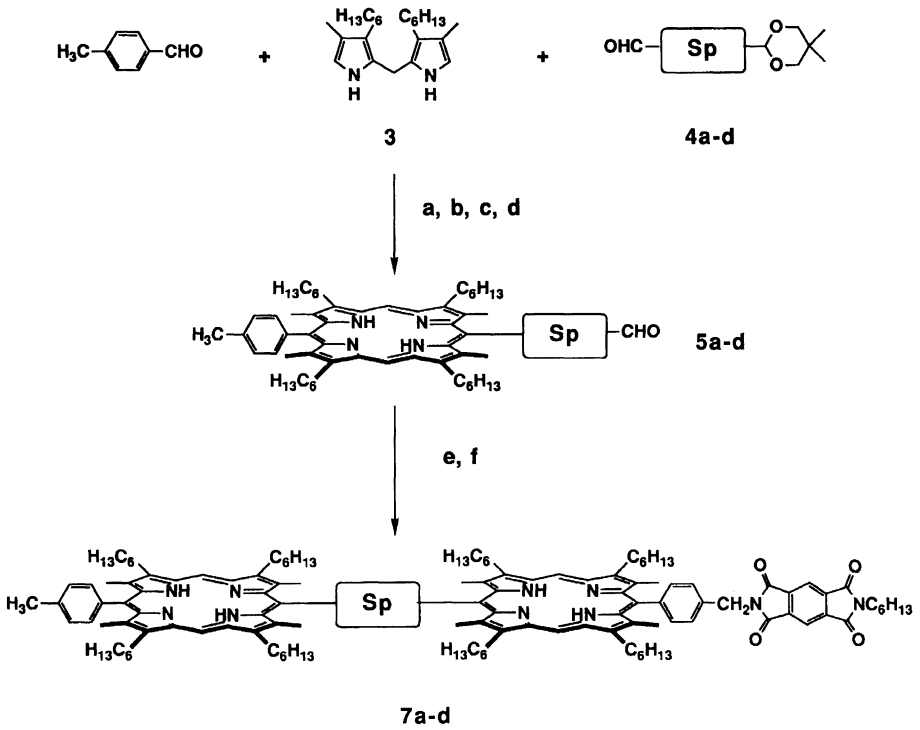

Scheme 2. Synthesis of **7a**—**d**: a, CCl_3CO_2H, CH_3CN, r. t., 15 h; b, *p*-chloranil, THF, r. t., 5 h; c, $Zn(OAc)_2$, MeOH, reflux, 1 h; d, 10% H_2SO_4, CF_3CO_2H, CH_2Cl_2, reflux, 10 h, e, **3**, (3 equivalent), **6** (2 equivalent), CCl_3CO_2H, CH_3CN, r. t., 5 h; f, *p*-chloranil, THF, r. t., 5 h.

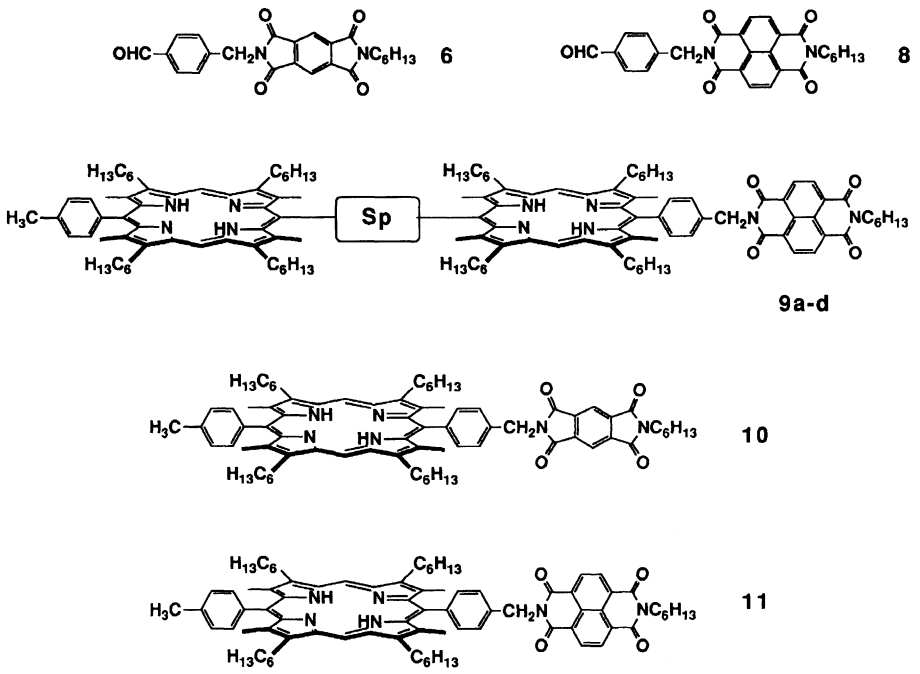

Chart 2. Structures of **6**, **8**, **9a**—**d**, **10**, and **11**.

umn chromatography. We first attempted the condensation of the zinc complex of **5a** and **6** with **3** under the same conditions used for **7** and **9**, but under these conditions undersired demetalation of zinc ion took place during the reaction. However, we found that **1a** was synthesized in an acceptable yield (10%) with aid of a catalytic amount of trichloroacetic acid (see Experimental Section). This finding seems to be of significant synthetic importance since partially zinc-metalated di- or oligoporphyrins could be prepared by this strategy.

Optical Properties. The absorption spectrum of **1b** is almost identical to the sum of those of monomeric ZnP and H_2P. Virtually the same spectra were also observed for **1c**, **d** and **2b**—**d**. On the other hand,

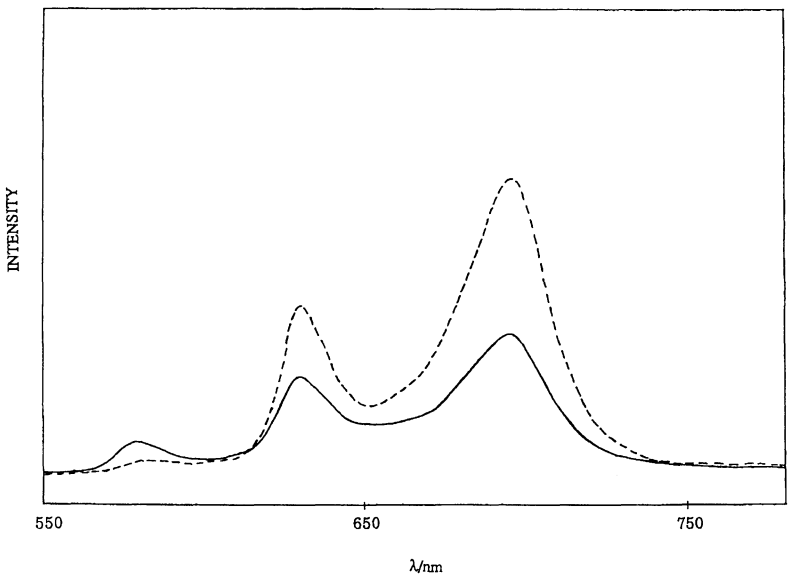

Fig. 1. Fluorescence spectra of two monozinc complexes of diporphyrins in THF; (—) for the major isomer and (- - -) for the minor one.

the Soret bands of 1,4-phenylene-bridged models **1a** and **2a** were rather broadened and the Q bands were slightly shifted (1—3 nm), indicating substantial exciton coupling of the ZnP and H_2P moieties. Figure 2 shows the steady-state fluorescence spectra of **1a**—**d** in THF. The spectra were composed of fluorescence emission from the respective chromophores. Owing to the existence of the intramolecular singlet-singlet energy-transfer process (step 3 in Scheme 1), the fluorescence intensity of the ZnP is reduced and that of the H_2P is enhanced. Intramolecular charge separation reaction between the $^1(H_2P)^*$ and PIm (step 4 in Scheme 1) reduced the emission intensity due to the $^1(H_2P)^*$. In a set of analogous acceptor-free models, the rates of the intramolecular singlet-singlet energy transfer have been reported to be 5.9×10^{10}, 5.7×10^9, and 6.4×10^9 s^{-1} for 1,4-phenylene-, 4,4′-biphenylylene-, and methylenebis(1,4-phenylene)-bridged one, respectively.[11] It may be reasonable to assume similar rates for the energy transfer in **1a**—**c**.[18] A much smaller rate for the energy transfer is expected for **1d**, since the center-to-center distance between the ZnP and H_2P is much longer. These expectations are consistent with the fluorescence spectra in Fig. 2, since the the fluorescence intensity of the ZnP decreases in the order of **1d**>**1b**>**1c**>**1a**. In the dyad **10**, the fluorescence lifetime of the H_2P is 5.2 ns in THF and thus the rate of the charge separation ($^1(H_2P)^*$–PIm→$(H_2P)^+$–$(PIm)^-$), k_{CS}, is estimated to be 1.1×10^8 s^{-1}.[17] Figure 3 shows the steady-state fluorescence spectra of **2a**—**d**. In these NIm-linked triads, the intramolecular charge separation (step 4 in Scheme 1) is more efficient in comparison with that in the PIm-linked triads. This comes from the fact that a NIm moiety is a stronger electron acceptor than PIm; one-electron reduction potentials of PIm and NIm in DMF are −1.24 and −0.99 V vs. ferrocene/ferrocenium ion, respectively. Indeed, in the reference model **11**, the fluorescenece lifetime is only 147 ps in THF and k_{CS} is thus calculated to be 6.7×10^9 s^{-1}. These results indicate that the quantum yield for the formation of ZnP–$(H_2P)^+$–$(NIm)^-$ from ZnP–$^1(H_2P)^*$–NIm is virtually quantitative, while the corresponding quantum yield in the PIm-bearing triads is only 0.58. Since the IP states $(ZnP)^+$–H_2P–$(PIm)^-$ and $(ZnP)^+$–H_2P–$(NIm)^-$ should be formed via the corresponding IP states ZnP–$(H_2P)^+$–$(PIm)^-$ and ZnP–$(H_2P)^+$–$(NIm)^-$, respectively, we may expect higher quantum yield for the formation of $(ZnP)^+$–H_2P–$(NIm)^-$ than $(ZnP)^+$–H_2P–$(PIm)^-$.[18]

Formation of Long-Lived Charge-Separated States. Photoexcitation of **1** or **2** leads to the formation of long-lived charge-separated states $(ZnP)^+$–H_2P–$(PIm)^-$ and $(ZnP)^+$–H_2P–$(NIm)^-$ probably via the reaction scheme shown in Scheme 1. Photoexcitation of the triads at 532 nm in THF solution leads to the population of $^1(ZnP)^*$–H_2P–Im and ZnP–$^1(H_2P)^*$–Im. Steps 1 and 2 involve all radiative and nonradiative decaying pathways to the ground states of ZnP and H_2P, respectively. Singlet-singlet excitation energy transfer occurs efficiently from the former to the latter (step 3) and subsequent charge separation between $^1(H_2P)^*$ and Im (step 4) results in the formation of ZnP–$(H_2P)^+$–$(Im)^-$, in which slightly exothermic hole transfer from the $(H_2P)^+$ to the ZnP moiety (step 6), in competition with an energy wasteful charge recombination to the ground state (step 5), finally leads to the generation of $(ZnP)^+$–H_2P–$(Im)^-$. Except for slow charge recombination in $(ZnP)^+$–H_2P–$(Im)^-$ (step 7), other energy-transfer and electron transfer reactions (step 3—6) should occur on picosecond to hundred picoseconds time scale and these reactions were indeed observed by picosecond transient absorp-

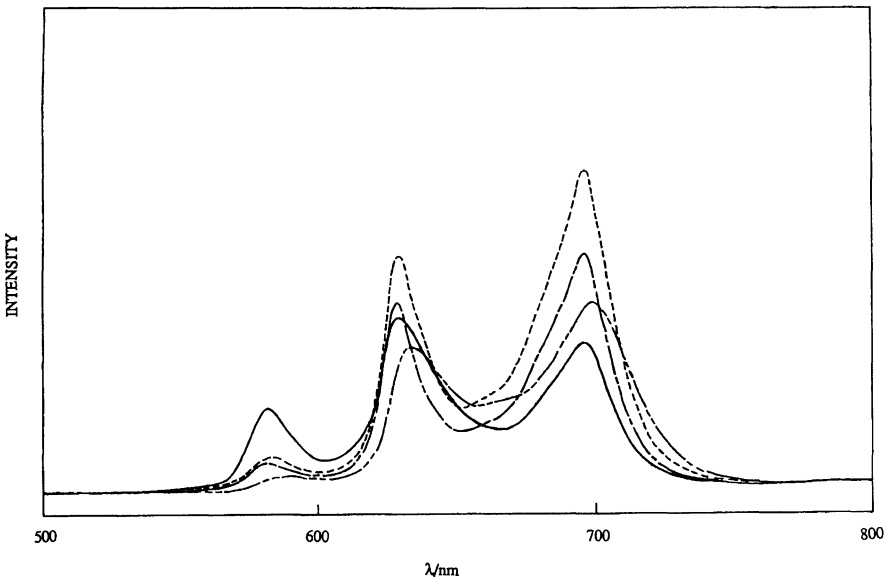

Fig. 2. Fluoresence spectra of **1a**—**d** in THF for excitation at the respective Soret band. The absorbances at the exciting wavelength were adjusted at 0.3. **1a**(–··–), **1b**(– – –), **1c**(–·–), and **1d**(——).

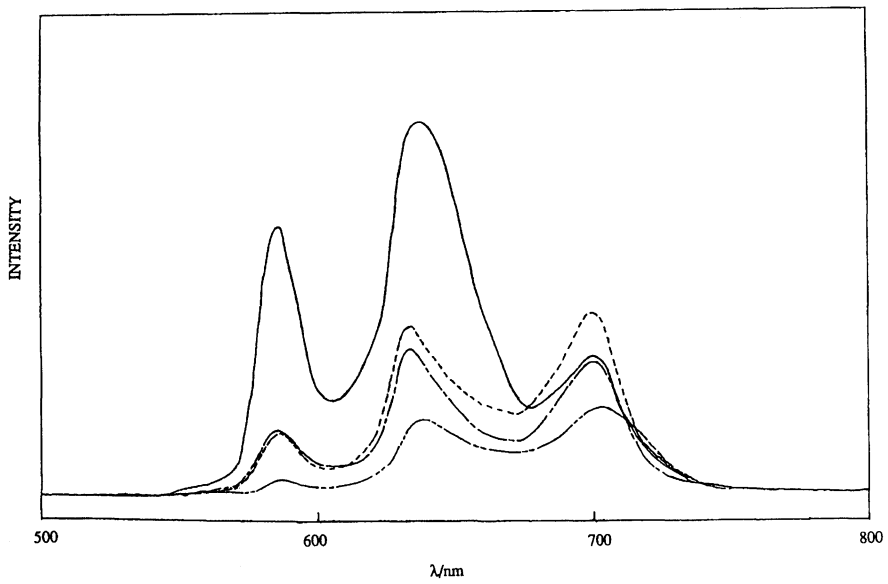

Fig. 3. Fluoresence spectra of **2a**—**d** in THF for excitation at the respective Soret band. The absorbances at the exciting wavelength were adjusted at 0.3. **2a**(–··–), **2b**(– – –), **2c**(–·–), and **2d**(——).

tion spectroscopy.[7,18] In this paper, however, we only discuss the charge-recombination reaction in the final IP states, $(ZnP)^+$–H_2P–$(Im)^-$, which proceeds on several hundreds nanosecond to microsecond time scale. Figures 4 and 5 show the nanosecond to microsecond transient absorption spectra of **1b** and **2b** in THF for excitation at 532 nm. In the transient absorption spectrum of **1b** at 200 ns, the absorbances at 670 and 715 nm were assigned to $(ZnP)^+$ and $(PIm)^-$, respectively, on the basis of the relevant absorption spectra.[12] Bleaching at 540 mn also indicated the formation of $(ZnP)^+$. In the absorption spectrum at 4 μs, we observed rather broad absorbance from 580 to 800 nm, assignable to $^3(H_2P)^*$, which decays with a lifetime of 14 μs. By tracing the absorbance at 715 nm, we have determined the lifetime of $(ZnP)^+$–H_2P–$(PIm)^-$ in **1b** to be 0.46 μs. On the other hand, $(NIm)^-$ generated by electrochemical reduction in DMF, shows absorption bands at 608 (ε=8960), 682 (3650), and 756 (6370) nm. The $(ZnP)^+$ species has a molar extinction coefficient more than 10000 at 670 nm. Therefore, the transient absorption spectrum of **2b** at 200 ns can be interpreted mainly due to $(ZnP)^+$–H_2P–$(NIm)^-$ contaminated with a small amount of $^3(H_2P)^*$. Thus by tracing the characteristic bands due to $(NIm)^-$, we have determined the lifetime of $(ZnP)^+$–H_2P–$(NIm)^-$ to be 1.1 μs. The

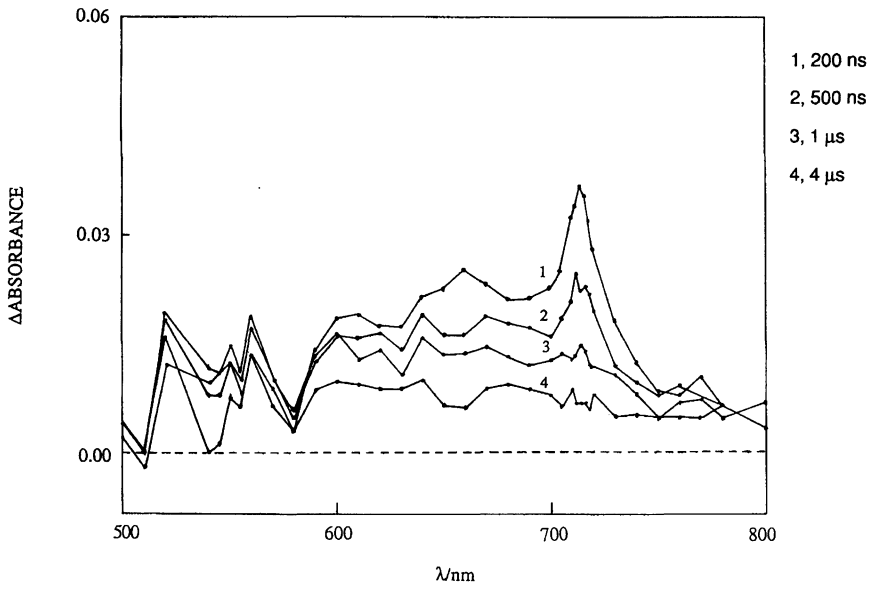

Fig. 4. Transient absorption spectra of **1b** in THF for excitation at 532 nm.

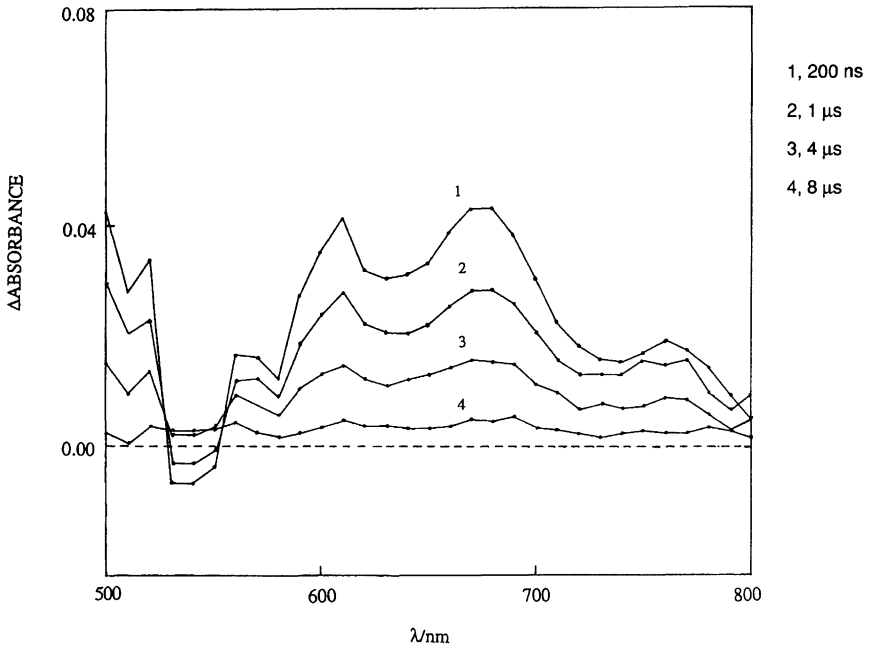

Fig. 5. Transient absorption spectra of **2b** in THF for excitation at 532 nm.

lifetimes of the final IP states thus determined are 3.0 and 4.5 μs for **1c** and **2c**. In **1d** and **2d**, where the ZnP and H_2P moieties are bridged by a bicyclo[2.2.2]octane spacer, the amounts of the $(ZnP)^+$–H_2P–$(Im)^-$ states are quite small and the absorptions due to the IP states are almost buried in the absorption due to $^3(ZnP)^*$. Therefore, the lifetimes of the $(ZnP)^+$–H_2P–$(Im)^-$ in **1d** and **2d** were determined to be both more than 80 μs under oxygen bubbling conditions. The lifetime of $(ZnP)^+$–H_2P–$(PIm)^-$ in **1d** was found to become increasingly longer upon lowering the temperature and to reach to 1 ms at −90 °C in a mixture of THF and butyronitrile (1 : 1). In the 1,4-phenylene-bridged models **1a** and **2a**, the decays of the transient absorptions due to the $(ZnP)^+$–H_2P–$(Im)^-$ were found to follow biphasic kinetics; 40 and 140 ns for **1a** and 10—20 and 200 ns for **2a**. The reason for this remains to be clarified yet. However, it seems likely that in the $(ZnP)^+$–H_2P–$(Im)^-$ IP states the rate of singlet-triplet intersystem crossing may compete with the charge recombination to the ground state. It is interesting to note that the lifetime of $(ZnP)^+$–H_2P–$(PIm)^-$ is shorter than that of the corresponding $(ZnP)^+$–H_2P–$(NIm)^-$ bearing the same bridge between the ZnP and H_2P moieties. Thus the charge-recombination process in $(D_1)^+$–D_2–$(A)^-$ is more efficient in models with a larger energy gap between the IP states and ground states. This is in contrast to the well-characterized behaviors of charge-

recombination process in simple, covalently-linked 1 : 1 $(donor)^+$–$(acceptor)^-$ ion pairs, since in such dyads, only the inverted behavior has been revealed so far for the charge recombination process.[12,19]

In summary, the relatively long-lived charge-separated states are generated upon excitation of conformationally restricted ZnP–H_2P–Im triads in THF via the sequential energy- and electron-transfer reactions: $^1(ZnP)^*$–H_2P–Im→ZnP–$^1(H_2P)^*$–Im→ZnP–$(H_2P)^+$–$(Im)^-$→$(ZnP)^+$–H_2P–$(Im)^-$. As long as 80 μs lifetime was indeed realized in the triads with a bicyclo[2.2.2]octyl-1,4-bis(1,4-phenylene) bridge between the ZnP and H_2P. The charge recombination reaction in the final $(ZnP)^+$–H_2P–$(PIm)^-$ state is slightly faster than that in the corresponding $(ZnP)^+$–H_2P–$(NIm)^-$ bearing the same bridge. Several advantages in the use of PIm and NIm as an electron acceptor are evident through this study; 1) the diimide-linked porphyrins are remarkably stable and easily manipulated in comparison with the corresponding quinone-linked porphyrin models, 2) the PIm and NIm moieties are particularly useful in the study of electron-transfer kinetics owing to the strong and characteristic absorptions of their anion radicals. On the basis of the present results, further works directed toward achieving longer-lived IP states via more efficient sequential electron-transfer reactions are currently in progress.

Experimental

Unless otherwise stated, all commercially availabel solvents and reagents were used without further purification. Acetonitrile, THF, and CH_2Cl_2 for synthetic use were refluxed over and distilled from P_2O_5, sodium benzophenone ketyl, and CaH_2, respectively. DMF was distilled under reduced pressure and stored over molecular sieves for several days before use. Melting points were measured on a Yanagimoto micro melting-point apparatus and are uncorrected.

UV-visible spectra were obtained with a Shimadzu UV-3000 spectrometer. Steady-state fluorescence spectra were taken on a Shimadzu RF-502A spectrofluorimeter. ^{1}H NMR spectra were recorded on a JEOL GX-400 spectrometer. Chemical shifts were reported in the δ scale (ppm) relative to internal Me_4Si. Mass spectra of the porphyrin compounds were recorded on a JEOL HX-110 spectrometer using the positive FAB (fast atom bombardment) ionization method (accelerating voltages 1.5 and 10 kV, Xe atom as the primary ion source). The FAB matrix was 3-nitrobenzyl alcohol/chloroform. A Q-switched Nd^{3+} : YAG laser (Quantel YG580) with second harmonic outpur (532 nm, 15-ns pulse duration) of 40 mJ was used for measurements of transient absorption spectra.[20]

The syntheses of **4a—c** and **6** were described elsewhere.[14] The aldehyde **4d** was prepared from 1,4-diphenylbicyclo-[2.2.2]octane[21] in 4 steps. 1,4-Diphenylbicyclo[2.2.2]octane (3.0 g, 11.5 mmol) was dissolved in CCl_4 (150 ml). To this solution iron powder (130 mg) was added, and later a solution of bromine (1.16 ml) in CCl_4 (100 ml) was added. The resulting reaction mixture was refluxed for 1.5 h. After being cooled, the mixture was poured into 10% NaOH solution, and was extracted with $CHCl_3$. The organic layers were combined and dried over anhydrous Na_2SO_4. The solvent was removed by the rotary evaporator. The residue was recrystallized from hexane to give 1,4-bis(4-bromophenyl)-bicylo[2.2.2]octane (2.91 g, 63%, yellowish crystals). Mp> 300°C; ^{1}H NMR ($CDCl_3$) δ=7.42 (4H, d, J=8.6 Hz), 7.24 (4H, d, J=8.6 Hz), and 1.93 (12H, s, Octane). The dibromide obtained (1.0 g, 2.4 mmol) was dissolved in dry THF (100 ml). To this solution, n-BuLi (1.6 mol dm^{-3} solution in hexane, 2.4 ml) was added dropwise over 10 min (−78 °C, under N_2). The reaction mixture was stirred for 1 h, and DMF (5 ml) was added, and the resulting reaction mixture was stirred further for 30 min. Then the reaction mixture was poured into water, and extracted with ethyl acetate. The extracts were combined, washed with 1 equiv HCl and water, and dried over anhydrous Na_2SO_4. The solvent was removed by the rotary evaporator. The residue obtained was refluxed in benzene (200 ml) in the presence of 2,2-dimethyl-1,3-propanediol (0.27 g, 2.6 mmol) and p-toluenesulfonic acid (0.045 g, 0.12 mmol) for 4 h. The reaction mixture was cooled and worked-up in the usual manner. The residue was separated by column chromatography (silica gel, CH_2Cl_2). The second fraction was collected (0.45 g) and treated with n-BuLi and DMF as described above. After usual workup, the product was recrystallized form hexane to give the pure compound **4d**. Yield 33%, mp>300°C. ^{1}H NMR ($CDCl_3$) δ=9.99 (1H, s, CHO), 7.83 (2H, d, J=8.2 Hz), 7.53 (2H, d, J=8.2 Hz), 7.46 (2H, d, J=8.6 Hz), 7.37 (2H, d, J=8.6 Hz), 5.38 (1H, s), 3.77 (2H, d, J=11 Hz), 3.63 (2H, d, J=11 Hz), 1.99 (12H, s), 1.30 (3H, s), and 0.80 (3H, s). MS (FAB) m/z 405 (M^+). Found C, 79.93; H, 8.10%. Calcd for $C_{27}H_{32}O_3$: C, 80.16; H, 7.97%.

***N*- Hexyl- *N'*- [(4- formylphenyl)methyl]- 1, 4 : 5, 8-naphthalenetetracarboximide (8).** To a solution of 4-(5,5-dimethyl-1,3-dioxan-2-yl)benzylamine[14] (1.11 g, 5 mmol) and hexylamine (0.51 g, 5 mmol) in DMF (60 ml) was added a solution of 1,4 : 5,8-naphthalenetetracarboxylic dianhydride (1.34 g, 5 mmol) in DMF (40 ml) at room temperature. The mixture was heated to 120 °C for 5 h and cooled to room temperature. The precipitates formed, which were collected by filtration, contained three diimide products. The second eluting fraction was separated by column chromatography (silica gel, CH_2Cl_2). The solvent was removed by the rotary evaporator. This product (1.07 g, 2.0 mmol, 40%) was treated with acid to hydrolyze the acetal protecting group (CH_2Cl_2 50 ml, trifluoroacetic acid 10 ml, 10% aq H_2SO_4 10 ml, room temperature, overnight). The reaction mixture was poured into water. The organic layer was separated, washed with $NaHCO_3$ solution and water, and dried. The solvent was removed by the rotary evaporator. Yield (0.89 g, 40%), mp 263—264 °C. ^{1}H NMR ($CDCl_3$) δ=9.98 (1H, s, CHO), 8.78 (4H, m, NIm-H), 7.84 (2H, d, J=8.2 Hz), 7.69 (2H, d, J=8.2 Hz), 5.47 (2H, s, $-CH_2-$), 4.22 (2H, t, $\underline{CH_2}(CH_2)_4CH_3$, J=7.3 Hz), 1.20—1.75 (8H, m, $CH_2(\underline{CH_2})_4CH_3$), 0.90 (3H, t, $(CH_2)_5\underline{CH_3}$, J=7.3 Hz). MS (FAB) m/z 468 (M^+). Found: C, 71.81; H, 5.16; N, 5.95%. Calcd for $C_{28}H_{24}N_{12}O_5$: C, 71.78; H, 5.16; N, 5.98%.

Synthesis of Formyl-Substituted Monomeric Porphyrins 5a—d. The synthesis of **5a** is described here as a typical procedure. p-Tolualdehyde (0.06 g, 0.5 mmol),

the aldehyde **4a** (0.11 g, 0.5 mmol), and **3** (0.34 g, 1 mmol) were dissolved in dry acetonitrile (15 ml). To this solution was added a solution of trichloroacetic acid (0.02 g) in acetonitrile (0.5 ml). The resulting mixture was stirred in the dark for 15 h at room temperature under nitrogen. Then a solution of *p*-chloranil (0.23 g, 1.5 mmol) in THF (10 ml) was added, and the solution was stirred for an additional 5 h. The solvent was removed by the rotary evaporator. The residue was dissolved in chloroform, washed with aq $NaHCO_3$ and water, and dried over anhydrous Na_2SO_4. To this solution was added a MeOH solution of $Zn(OAc)_2$, and the resulting mixture was refluxed for 1 h. After being cooled, the reaction mixture was washed with water, and the organic layer was separated, dried over Na_2SO_4, and evaporated. Separation on silica gel ($CHCl_3$ as eluent) afforded zinc complex of desired cross-coupling porphyrin (0.17 g), which was dissolved in a mixture of trifluoroacetic acid (3 ml), 10% H_2SO_4 (3 ml), and CH_2Cl_2 (20 ml). After being refluxed for 10 h, the mixture was poured into water, washed with aq $NaHCO_3$ and water, and extracted with CH_2Cl_2. The organic layers were combined and dried over Na_2SO_4. The solvent was removed by the rotary evaporator. The residue was trituated with methanol to give the porphyrin **5a**: Yield 31%. ^{1}H NMR ($CDCl_3$) δ=10.40 (1H, s, CHO), 10.24 (2H, s, meso), 8.28 (4H, d, J=3.4 Hz), 7.92 (2H, d, J=7.8 Hz), 7.54 (2H, d, J=8.3 Hz), 4.00 (8H, t, $\underline{CH_2}(CH_2)_4CH_3$, J=7.3 Hz), 2.72 (3H, s, Ar-$\underline{Me}$), 2.51 (6H, s, Me), 2.45 (6H, s, Me), 1.25—2.30 (32H, m, $CH_2(\underline{CH_2})_4CH_3$), 0.89 (12H, t, $(CH_2)_5\underline{CH_3}$, J=7.3 Hz), and −2.38 (2H, broad, NH). MS (FAB) H_2P m/z 897 (M^++1); ZnP m/z 960 (M^++1).

The compounds **5b**—**d** were prepared in the similar manner as **5a**. Only the chemical yields and the physical properties are listed below:

5b: Yield (2 steps, 28%). ^{1}H NMR ($CDCl_3$) δ= 10.24 (2H, s, meso), 10.18 (1H, s, CHO), 8.18 (2H, d, J=8.3 Hz), 8.13 (4H, s, biPh), 8.04 (2H, d, J=8.3 Hz), 7.92 (2H, d, J=7.8 Hz), 7.53 (2H, d, J=8.3 Hz), 4.01 (8H, t, $\underline{CH_2}(CH_2)_4CH_3$, J=7.3 Hz), 2.72 (3H, s, Ar-$\underline{Me}$), 2.55 (6H, s, Me), 2.51 (6H, s, Me), 1.25—2.30 (32H, m, $CH_2(\underline{CH_2})_4CH_3$), 0.89 (12H, t, $(CH_2)_5\underline{CH_3}$, J=7.3 Hz), and −2.38 (2H, broad, NH). MS (FAB) H_2P m/z 974 (M^++2).

5c: Yield (2 steps, 25%). ^{1}H NMR ($CDCl_3$) δ=10.24 (2H, s, meso), 10.09 (1H, s, CHO), 8.01 (1H, d, J=7.8 Hz), 7.99 (1H, d, J=7.8 Hz), 7.96 (1H, d, J=6.8 Hz), 7.93 (1H, d, J=6.8 Hz), 7.59 (2H, d, J=8.3 Hz), 7.55 (2H, d, J=7.8 Hz), 7.37 (2H, s, Ar-H), 7.26 (2H, s, Ar-H), 4.41 (2H, s, $-CH_2-$), 4.01 (8H, t, $\underline{CH_2}(CH_2)_4CH_3$, J=7.3 Hz), 2.73 (3H, s, Ar-$\underline{Me}$), 2.52 (6H, s, Me), 2.51 (6H, s, Me), 1.25—2.30 (32H, m, $CH_2(\underline{CH_2})_4CH_3$), 0.92 (12H, t, $(CH_2)_5\underline{CH_3}$, J=7.3 Hz), and −2.35 (2H, broad, NH). MS (FAB) H_2P m/z 988 (M^++2).

5d: Yield (2 steps, 22%). ^{1}H NMR ($CDCl_3$) δ=10.23 (2H, s, meso), 10.04 (1H, s, CHO), 7.98 (2H, d, J=8.3 Hz), 7.94 (2H, d, J=7.8 Hz), 7.90 (2H, d, J=8.3 Hz), 7.67 (2H, d, J=8.3 Hz), 7.65 (2H, d, J=8.3 Hz), 7.54 (2H, d, J=7.8 Hz), 4.01 (8H, t, $\underline{CH_2}(CH_2)_4CH_3$, J=7.3 Hz), 2.72 (3H, s, Ar-$\underline{Me}$), 2.54 (6H, s, Me), 2.51 (6H, s, Me), 1.25—2.30 (32H, m, $CH_2(\underline{CH_2})_4CH_3$), 0.89 (12H, t, $(CH_2)_5\underline{CH_3}$, and bicyclo-[2.2.2]octyl, J=7.3 Hz), and −2.36 (2H, broad, NH). MS (FAB) H_2P m/z 1082 (M^++2).

Synthesis of Pyromellitimide-Linked Monozinc Complex of Diporphyrin 1a. The zinc complex of formyl-substituted porphyrin **5a** (13.6 mg, 14.1 μmol) and the *N*-(formylphenylmethyl)substituted diimide **6** (11.8 mg, 28.2 μmol) and were dissolved in a mixture of dry acetonitrile (5 ml) and dry chloroform (5 ml) containing trichloroacetic acid (7.6 mg, 46.5 μmol). To this solution, dipyrrolylmethane **3** (22.0 mg, 42.3 μmol) in dry acetonitrile (5 ml) was added, and the mixture was stirred for 5 h at room temperature under nitrogen. Then a solution of *p*-chloranil (37 mg) in THF (10 ml) was added, and the solution was stirred further for 5 h. The solvent was evaporated and the residue was taken up in chloroform, washed with aq $NaHCO_3$ and water, the organic layer was dried over Na_2SO_4 and evaporated. The produced monozinc complex of **1a** were separated by column chromatography on silica gel, and recrystallized from MeOH. Yield 10%. ^{1}H NMR ($CDCl_3$) δ=10.26 (4H, s, meso), 8.68 (4H, s, sp-Ar-H), 8.10 (2H, s, Im-H), 7.77 (2H, d, J=7.8 Hz), 7.72 (2H, d, J=8.8 Hz), 7.62 (2H, d, J=7.8 Hz), 7.54 (2H, d, J=8.8 Hz), 5.54 (2H, s, $-CH_2-$), 4.03 (18H, m, $\underline{CH_2}(CH_2)_4CH_3$), 3.27 (6H, s, Me), 3.23 (6H, s, Me), 2.76 (3H, s, Ar-$\underline{Me}$), 2.56 (6H, s, Me), 2.41 (6H, s, Me), 1.50—2.30 (72H, m, $CH_2(\underline{CH_2})_4CH_3$), 0.70—1.00 (27H, m, $(CH_2)_5\underline{CH_3}$), −2.28 (1H, broad, NH), −2.42 (1H, broad, NH). MS (FAB) ZnP–H_2P–PIm m/z 2021 (M^++2), UV-vis λ_{max} 422 (1000), 504.5 (166), 542 (173), 579.5 (144), 632 nm (120).

Monozinc complex of 1,4:5,8-naphthalenetetracarboximide-linked diporphyrin **2a** was prepared in the similar manner as **1a**. Only the chemical yields and the compound data are listed below:

2a: Yield 32%. ^{1}H NMR ($CDCl_3$) δ=10.24 (4H, s, meso), 8.68 (4H, s, sp-Ar-H), 8.06 (4H, d, J=7.8 Hz), 7.77 (2H, d, J=7.8 Hz), 7.72 (2H, d, J=8.8 Hz), 7.62 (2H, d, J=7.8 Hz), 7.55 (2H, d, J=8.8 Hz), 5.55 (2H, s, $-CH_2-$), 4.04 (18H, m, $\underline{CH_2}(CH_2)_4CH_3$), 3.28 (6H, s, Me), 3.23 (6H, s, Me), 2.78 (3H, s, Ar-$\underline{Me}$), 2.56 (6H, s, Me), 2.41 (6H, s, Me), 1.50—2.30 (72H, m, $CH_2(\underline{CH_2})_4CH_3$), 0.70—1.00 (27H, m, $(CH_2)_5\underline{CH_3}$), −2.25 (1H, broad, NH), −2.40 (1H, broad, NH). MS (FAB) ZnP–H_2P–NIm m/z 2071 (M^++2), UV-vis λ_{max} 423.5 (1000), 508 (165), 544.5 (169), 577.5 (153), 628 nm (122).

Synthesis of Pyromellitimide-Linked Diporphyrin 7b. The porphyrin **5b** (20.7 mg, 0.02 mmol) and the diimide **6** (16.7 mg, 0.04 mmol) were dissolved in a mixture of acetonitrile (7 ml) and CH_2Cl_2 (6 ml) containing trichloroacetic acid (3.6 mg, 0.02 mmol). To this solution, the dipyrrolylmethane **3** (20.5 mg, 0.06 mmol) in acetonitrile (5 ml) was added, and the mixture was stirred for 5 h at room temperature under nitrogen. Then a solution of *p*-chloranil (23.2 mg) in THF (10 ml) was added, and the solution was stirred further for 5 h. The volatile solvent was removed by the rotary evaporator. The residue was dissolved in $CHCl_3$, and the resulting solution was washed with aq $NaHCO_3$ and water. To this solution was added a MeOH solution of $Zn(OAc)_2$, and the resulting mixture was refluxed for 1 h. After being cooled, the reaction mixture was washed with water, and the organic layer was separated, dried over Na_2SO_4. The solvent was removed by the rotary evaporator. Separation on silica-gel column ($CHCl_3$) gave bis-zinc complex of **7b**, which was converted to **7b** on treatment with 4 M hydrochloric acid (1 M=1 mol dm^{-3}). Yield 29%. ^{1}H NMR ($CDCl_3$) δ=10.28 (4H, s, meso), 8.31 (4H, s, biph), 8.07 (2H, d, J=8.3 Hz), 8.06

(2H, s, PIm-H), 7.97 (2H, d, J=7.8 Hz), 7.73 (2H, d, J=7.8 Hz), 7.56 (2H, d, J=7.8 Hz), 5.15 (2H, s, $-CH_2-$), 4.01 (18H, m, $\underline{CH_2}(CH_2)_4CH_3$), 2.73 (3H, s, Ar-$\underline{Me}$), 2.73 (6H, s, Me), 2.72 (6H, s, Me), 2.54 (6H, s, Me), 2.43 (6H, s, Me), 1.50—2.30 (72H, m, $CH_2(\underline{CH_2})_4CH_3$), 0.70—1.00 (27H, m, $(CH_2)_5\underline{CH_3}$), −2.35 (2H, broad, NH). MS (FAB) H_2P–H_2P–PIm m/z 2034 (M^++2); ZnP–H_2P–PIm m/z 2098 (M^++3), UV-vis λ_{max} 418.5 (1000), 505 (156), 544 (157), 577.5 (138), 624 nm (107).

The compounds **7c—d** and **9b—d** were prepared in the similar manner as **7b**. Only the chemical yields and the physical properties are listed below:

7c: Yield 45%. ^{1}H NMR ($CDCl_3$) δ=10.25 (4H, s, meso), 8.16 (2H, d, J=2.9 Hz), 8.14 (2H, d, J=2.9 Hz), 8.11 (2H, d, PIm-$\underline{H}$), 8.05 (4H, d, J=7.8 Hz), 7.96 (2H, d, J=7.8 Hz), 7.85 (4H, d, J=7.8 Hz), 7.73 (2H, d, J=7.8 Hz), 7.56 (2H, d, J=7.8 Hz), 5.19 (2H, s, $-CH_2-$), 4.72 (2H, s, Ar–$\underline{CH_2}$–Ar), 4.01 (18H, m, $\underline{CH_2}(CH_2)_4CH_3$), 2.74 (3H, s, Ar-$\underline{Me}$), 2.64 (12H, s, Me), 2.53 (6H, s, Me), 2.43 (6H, s, Me), 1.50—2.30 (72H, m, $CH_2(\underline{CH_2})_4CH_3$), 0.70—1.00 (27H, m, $(CH_2)_5\underline{CH_3}$), −2.38 (2H, broad, NH). MS (FAB) H_2P–H_2P–PIm m/z 2048 (M^++2), ZnP–H_2P–PIm m/z 2110 (M^++1), UV-vis λ_{max} 416.5 (1000), 503 (141), 546.5 (137), 577 (125), 626 nm (101).

7d: Yield 7%. ^{1}H NMR ($CDCl_3$) δ=10.20 (4H, s, meso), 8.36 (2H, s), 8.08 (2H, d, J=7.8 Hz), 8.06 (2H, d, J=8.3 Hz), 8.02 (2H, d, J=8.3 Hz), 7.95 (2H, d, J=7.8 Hz), 7.83 (4H, m), 7.74 (2H, d, J=6.8 Hz), 7.54 (2H, d, J=7.8 Hz), 5.25 (2H, s, $-CH_2-$), 4.00 (18H, m, $\underline{CH_2}(CH_2)_4CH_3$), 2.73 (3H, s, Ar-$\underline{Me}$), 2.52 (6H, s, Me), 2.50 (6H, s, Me), 2.47 (6H, s, Me), 2.39 (6H, s, Me), 2.19 (12H, s, Oct-H), 1.50—2.30 (72H, m, $CH_2(\underline{CH_2})_4CH_3$), 0.70—1.00 (27H, m, $(CH_2)_5\underline{CH_3}$), −2.65 (2H, broad, NH). MS (FAB) H_2P–H_2P–PIm m/z 2143 (M^++3), ZnP–H_2P–PIm m/z 2206 (M^++3), UV-vis λ_{max} 416 (1000), 504.5 (86), 544.5 (86), 544.5 (91), 576.5 (75), 628 nm (53).

9b: Yield 22%. ^{1}H NMR ($CDCl_3$) δ=10.22 (4H, s, meso), 8.36 (4H, d, J=8.6 Hz), 8.31 (4H, d, J=8.6 Hz), 8.09 (4H, m), 8.01 (2H, d, J=8.3 Hz), 7.98 (2H, d, J=8.3 Hz), 7.74 (2H, d, J=8.3 Hz), 7.56 (2H, d, J=8.3 Hz), 5.53 (2H, s, $-CH_2-$), 4.03 (18H, m, $\underline{CH_2}(CH_2)_4CH_3$), 2.75 (3H, s, Ar-$\underline{Me}$), 2.73 (6H, s, Me), 2.72 (6H, s, Me), 2.52 (6H, s, Me), 2.39 (6H, s, Me), 1.50—2.30 (72H, m, $CH_2(\underline{CH_2})_4CH_3$), 0.70—1.00 (27H, m, $(CH_2)_5\underline{CH_3}$), −2.27 (2H, broad, NH). MS (FAB) H_2P–H_2P–NIm m/z 2084 (M^++2), ZnP–H_2P–NIm m/z 2147 (M^++2), UV-vis λ_{max} 418.5 (1000), 506 (79), 544 (83), 576 (64), 631 nm (55).

9c: Yield 40%. ^{1}H NMR ($CDCl_3$) δ=10.23 (4H, s, meso), 8.22 (4H, d, J=7.8 Hz), 8.01 (4H, d, J=7.3 Hz), 7.88 (4H, d, J=7.8 Hz), 7.78 (3H, d, J=7.3 Hz), 7.73 (3H, d, J=7.3 Hz), 7.58 (2H, d, J=7.8 Hz), 5.53 (2H, s, $-CH_2-$), 4.74 (2H, s, Ar–$\underline{CH_2}$–Ar), 4.05 (18H, m, $\underline{CH_2}(CH_2)_4CH_3$), 2.75 (3H, s, Ar-$\underline{Me}$), 2.69 (6H, s, Me), 2.68 (6H, s, Me), 2.55 (6H, s, Me), 2.37 (6H, s, Me), 1.50—2.30 (72H, m, $CH_2(\underline{CH_2})_4CH_3$), 0.70—1.00 (27H, m, $(CH_2)_5\underline{CH_3}$), −2.66 (2H, broad, NH). MS (FAB) H_2P–H_2P–NIm m/z 2098 (M^++2), ZnP–H_2P–NIm m/z 2160 (M^++1), UV-vis λ_{max} 417 (1000), 506 (81), 542 (83), 576 (84), 630 nm (43).

9d: Yield 15%. ^{1}H NMR ($CDCl_3$) δ=10.21 (4H, s, meso), 8.09 (2H, d, J=7.8 Hz), 8.07 (2H, d, J=8.3 Hz), 8.01 (2H, d, J=8.3 Hz), 7.99 (2H, d, J=7.8 Hz), 7.84 (4H, m), 7.75 (2H, d, J=6.8 Hz), 7.57 (2H, d, J=7.8 Hz), 7.36 (4H, s, Ar), 5.57 (2H, s, $-CH_2-$), 4.02 (18H, m, $\underline{CH_2}(CH_2)_4CH_3$), 2.74 (3H, s, Ar-$\underline{Me}$), 2.56 (6H, s, Me), 2.54 (6H, s, Me), 2.47 (6H, s, Me), 2.37 (6H, s, Me), 2.18 (12H, s, Oct-H), 1.50—2.30 (72H, m, $CH_2(\underline{CH_2})_4CH_3$), 0.70—1.00 (27H, m, $(CH_2)_5\underline{CH_3}$), −2.67 (2H, broad, NH). MS (FAB) H_2P–H_2P–NIm m/z 2193 (M^++3), ZnP–H_2P–NIm m/z 2254 (M^++1), UV-vis λ_{max} 416 (1000), 503.5 (179), 543 (183), 576 (181), 632 nm (143).

This work was partially supported by a Grant-in-Aid for Specially Promoted Research No. 02102005 from the Ministry of Education, Science and Culture.

References

1) J. Deisenhofer, O. Epp, K. Miki, R. Huber, and H. Michel, *J. Mol. Biol.*, **180**, 385 (1984).

2) a) C. H. Chang, D. M. Tiede, J. Tang, J. Norris, and M. Schiffer, *FEBS Lett.*, **205**, 82 (1986); b) J. P. Allen, G. Feher, T. O. Yeates, H. Komiya, and D. C. Rees, *Proc. Natl. Acad. Sci. U. S. A.*, **84**, 5730 (1987).

3) C. Kirmaier and D. Holten, *Photosynth. Res.*, **13**, 225 (1987).

4) a) D. Gust and T. A. Moore, *Science*, **244**, 35 (1989); b) D. Gust, T. A. Moore, and A. L. Moore, *Acc. Chem. Res.*, **26**, 198 (1993); c) J. L. Sessler, M. R. Johnson, S. E. Creager, J. C. Fettinger, and J. A. Ibers, *J. Am. Chem. Soc.*, **112**, 9310 (1990).

5) M. R. Wasielewski, *Chem. Rev.*, **92**, 435 (1992); M. R. Wasielewski, M. P. Niemczyk, W. A. Svec, and E. B. Pewitt, *J. Am. Chem. Soc.*, **107**, 5562 (1985).

6) K. Maruyama and A. Osuka, *Pure Appl. Chem.*, **62**, 1511 (1990).

7) A part of the present work was preliminary reported: A. Osuka, T. Nagata, F. Kobayashi, R. P. Zhang, K. Maruyama, N. Mataga, T. Asahi, T. Ohno, and K. Nozaki, *Chem. Phys. Lett.*, **199**, 302 (1992).

8) J. A. Cowan and J. K. M. Sanders, *J. Chem. Soc., Perkin Trans. 1*, **1985**, 2435.

9) A. Osuka, S. Nakajima, K. Maruyama, N. Mataga, and T. Asahi, *Chem. Lett.*, **1991**, 1003.

10) A. Osuka, H. Yamada, K. Maruyama, N. Mataga, T. Asahi, I. Yamazaki, and Y. Nishimura, *Chem. Phys. Lett.*, **181**, 419 (1991).

11) A. Osuka, T. Nagata, K. Maruyama, N. Mataga, T. Asahi, I. Yamazaki, and Y. Nishimura, *Chem. Phys. Lett.*, **185**, 88 (1991).

12) A. Osuka, S. Nakajima, K. Marluyama, N. Mataga, T. Asahi, I. Yamazaki, Y. Nishimura, T. Ohno, and K. Nozaki, *J. Am. Chem. Soc.*, **115**, 4577 (1993).

13) A. Osuka, T. Nagata, F. Kobayashi, and K. Maruyama, *J. Heterocycl. Chem.*, **27**, 1657 (1990).

14) T. Nagata, *Bull. Chem. Soc. Jpn.*, **64**, 3005 (1991).

15) T. Nagata, A. Osuka, and K. Maruyama, *J. Am. Chem. Soc.*, **112**, 3054 (1990).

16) A. Osuka, K. Maruyama, I. Yamazaki, and N. Tamai, *Chem. Phys. Lett.*, **165**, 392 (1990).

17) The value of k_{CS} was calculated by the following equation; $k_{CS}=1/\tau-1/\tau_0$, where τ and τ_0 are the fluorescence lifetimes of **10** and a PIm-free H_2P, respectively.

18) The excited-state dynamics of these triads were

also studied by picosecond transient absorption spectroscopy. Singlet–singlet energy transfer occurs with rates being similar to the values described in the text. For **2a**, the quantum yield for the formation of $(ZnP)^+-H_2P-(NIm)^-$ and the rate of hole transfer $(ZnP-(H_2P)^+-(NIm)^- \rightarrow (ZnP)^+-H_2P)-(NIm)^-)$ were determined to be 0.79 and 5.4×10^{10} s^{-1}, respectively. A. Osuka, R. P. Zhang, K. Maruyama, N. Mataga, Y. Tanaka, and T. Okada, *Chem. Phys. Lett.*, in press.

19) T. Asahi, M. Ohkochi, R. Matsusaka, N. Mataga, R. P. Zhang, A. Osuka, and K. Maruyama, *J. Am. Chem. Soc.*, **115**, 5665 (1993), and references cited therein.

20) T. Ohno, A. Yoshimura, and N. Mataga, *J. Phys. Chem.*, **94**, 4871 (1990).

21) N. B. Chapman, S. Sotheeswaran, and K. J. Toyne, *J. Org. Chem.*, **35**, 917 (1970).